

Novel Fourier approach to digital holography

S. PAŚKO* and R. JÓ WICKI

Institute of Micromechanics and Photonics, Warsaw University of Technology,
8 Chodkiewicza Str., 02-525 Warsaw, Poland

A complete simulation procedure of the holographic process using Fourier approach is proposed. The algorithm elaborated allows determining the field distributions in the object and hologram Fresnel regions. To show some advantages of the method proposed one-dimensional computer simulations for a simple amplitude object case using Fresnel and Fourier holographic configurations are presented. The usefulness of the algorithm for image reconstruction from a hologram registered by CCD camera is demonstrated.

Keywords: digital holography, Fourier transformation.

1. Introduction

The first digital reconstruction of a holographic image was accomplished by Kronrod, Yaroslawskaa, and Merzlyakov [1,2]. Their calculations were based on the Fresnel approximation of the Kirchhoff integral. Unfortunately, at that time the laboratory equipment did not allow digital registration of holograms and the computer calculation power was insufficient to introduce the new idea into practice. Schnars and Jüptner proposed the setup for digital holography [3,4]. The holographic process was divided into two steps – the 1st registration of the hologram of an object with the aid of CCD camera realised on the laboratory stand and - the 2nd obtaining of the holographic image of the object registered by computer calculations. The most important advantage of such a process is absence wet processing connected with the photographic material development. The digital hologram can be stored and preliminary preprocessed as well. The preprocessing is usually done to remove the zero diffraction order of the reconstructing beam and other noises in the reconstructed image.

Generally, there are two methods to reconstruct digital holograms: Fresnel approximation and the convolution approach [3,4]. Both methods have different properties. In the convolution approach the zero diffraction order in the reconstructed image is omitted. Additionally, the pixel size is constant and independent of the image position. In consequence, the reconstructed object area is equal to CCD matrix area. When the object registered is larger than the CCD matrix dimension, the whole holographic image should be composed of several subimages, what constitutes an essential disadvantage of the method. In the Fresnel approach the pixel size is variable depending on the reconstruction

distance. Moreover, strong zero diffraction order may distort the image demanded. To obtain a clear reconstructed image some filtration should be performed.

In the paper, another approach based on the Fourier transformation is proposed. In fact, it is similar to the Fresnel approximation method. Additionally, the properties of a new reconstruction procedure are analogous to the Fresnel approximation approach. However, the form of equations used is adapted in the optical processes to both the registration and reconstruction steps. Due to analogies with optical phenomena, the approach proposed significantly simplifies the analyses of the two steps of the holographic process. The procedures corroborated using some numerical examples.

2. General relations

As it was stated in introduction, the first step of the digital holographic process is realised on a laboratory stand. We propose to start with analytical considerations of a complete holographic procedure. The analytical tools used for both the registration and the reconstruction are the same. Moreover, the analysis of the whole procedure makes possible to determine the influence of differences between the laboratory and computational steps.

2.1. Geometrical approach

In this section, for simplicity, the consideration is presented for one-dimensional case. The equations for two-dimensional case are similar and straightforward. The computational problems in both cases are the same as well.

Let $z_p(x_p)$ be the coordinate describing the object shape with respect to the plane π (Fig. 1). The complex amplitude at the point $P(x)$ of the hologram H, as the result of interference of the object reference waves can be described by the following equation

* e-mail: s.pasko@mchtr.pw.edu.pl

$$V_H = \frac{1}{N} \sum_{p=1}^N \left\{ \frac{V_p}{r_p} \exp[ik(r_p - S - r + S_r)] \right\} + \frac{V_0}{r} \exp(i\Delta), \quad (1)$$

where

$$r = S_r \sqrt{1 - 2 \frac{x \sin \alpha}{S_r} + \left(\frac{x}{S_r} \right)^2}, \quad (2)$$

$$r_p = (S - z_p) \sqrt{1 + \left(\frac{x - x_p}{S - z_p} \right)^2}, \quad (3)$$

are the distances RP and A_pP , respectively. V_p and V_0 are the amplitudes of the wave fronts generated by the points A_p and R at the distances $r_p = 1$ and $r = 1$, respectively. The sum is accomplished for all the object points A_p . The denotation of remaining parameters used in Eqs. (1), (2), and (3) is given in Fig. 1(a). Equation (1) is given in such a form as to decrease the calculated values of phase differences. The quantity Δ is related to unknown phase difference between both interfering beams. The intensity distribution registered by a CCD camera is given by

$$I_H = V_H V_H^*. \quad (4)$$

In order to reconstruct the holographic image, the hologram is illuminated by a wave generated by a virtual source R' [Fig. 1(b)]. The field distribution V_r at the hologram plane can be expressed by

$$V_r = \frac{V_{0r}}{r'} \exp[ik(r' - S')], \quad (5)$$

where V_{0r} is the wave amplitude at $r' = 1$. Its value depends on the source power. The distances r' and S' correspond to the distances r and S of the registration system, they are marked in Fig. 1(b) as well. Assuming linear response of the CCD camera the holographic field distribution generating the holographic image can be described by linear equation

$$V_{rH} = I_H V_r. \quad (6)$$

The field distribution at the holographic image plane can be found from

$$V'(x'_p) = \sum_x \frac{V_{rH}(x)}{r'_p(x)} \exp[ik(r'_p - S')]. \quad (7)$$

Due to small diffraction angles, what is the typical case of the digital holography, the above relations can be simplified putting $\sin \alpha \approx \alpha$, expanding the roots in Eqs. (2) and (3) into geometrical series or omitting amplitude

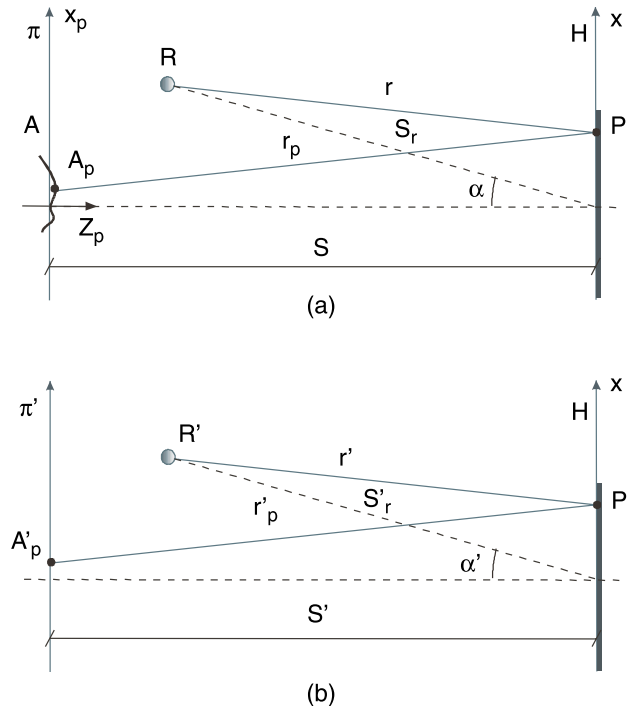


Fig. 1. Holographic registration (a) and reconstruction (b) configurations: A – object, R – centre of spherical wave front reference beam, H – hologram, R' – virtual point source of spherical wave front reconstructing beam.

changes in all terms of the type V/r [5]. All proposed simplifications accelerate the calculations. However, in all these cases the summations of the fields at the hologram plane or the image plane for two-dimensional system, or even one-dimensional one, are still time-consuming procedures.

2.2. Fourier transformation approach

We propose to change the above operations using the fast Fourier transformation. As it was mentioned in introduction our method is based on the optical description of the whole holographic process. In the method proposed the sphere theory based on Fourier transformation is applied [6]. Originally, this theory has been used to formulate the diffraction equations for the light propagation in the Fresnel's region. We would like to demonstrate that it can be applied to describe the whole holographic process. For that purpose the relation between two fields on two conjugate spheres will be used (Fig. 2). If $V(\rho)$ is the field distribution on the sphere Σ_0 with the centre at O_H , then the field distribution $V(A)$ on the sphere Σ_H with the centre at O_π can be found from the relation

$$V(A) = CFT^{-1}[V(\rho)], \quad (8)$$

where the parameterised linear co-ordinate at the hologram plane is

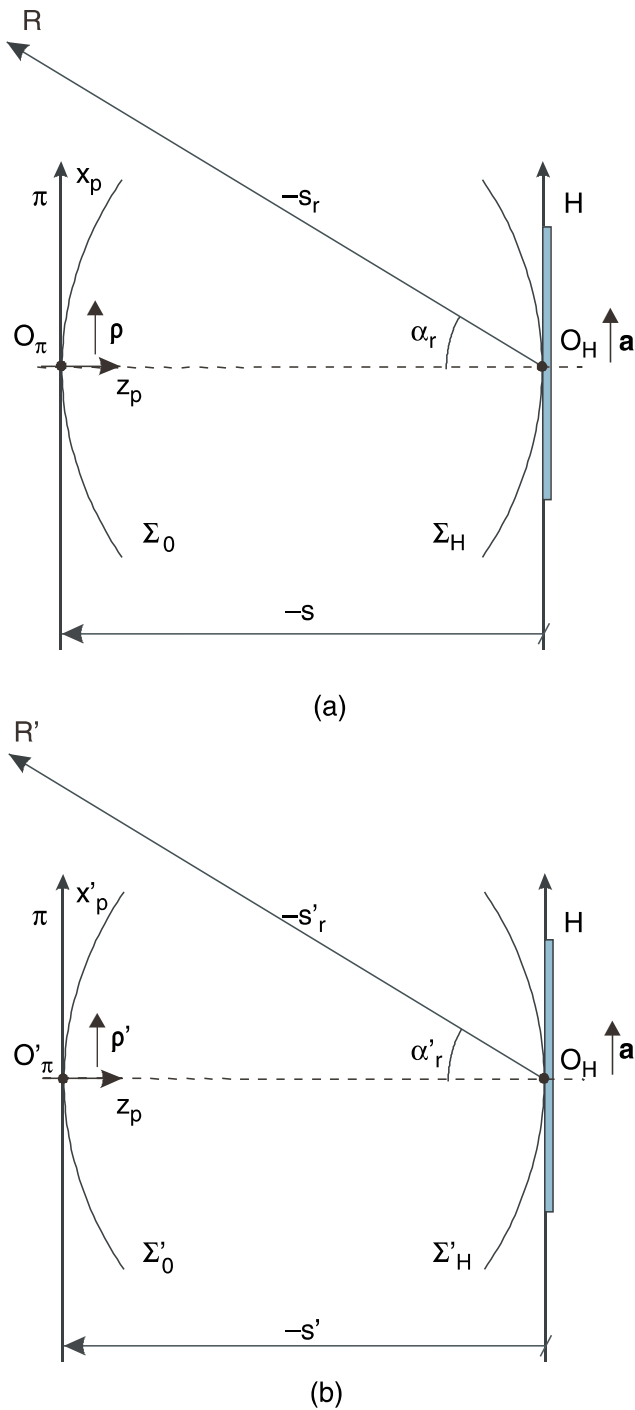


Fig. 3. Notations for hologram registration (a) and reconstruction (b) systems.

FT^+ denotes the inverse Fourier transformation operator. The relation between the parameterised coordinate A' and the linear coordinate a is described by [see Eq. (4), for comparison]

$$A' = -\frac{ka}{s'} \quad (21)$$

To prove the usefulness of the FFT approach, the proposed two cases of the holographic process will be consid-

ered. First, the full simulation for one-dimensional analysis of the hologram registration for a simple amplitude object and its image reconstruction will be presented. Next, in case of the reconstruction of its real image for the laboratory hologram registration will be determined.

3. Holographic process simulation using FFT

A chosen amplitude object is shown in Fig. 4. The phase in all its points is equal to zero. The object was divided into 1000 samples, the distance between the adjacent object pixels is equal to $\Delta x_p = 5 \mu\text{m}$. The remaining experiment parameters are: the light wavelength $\lambda = 0.6328 \mu\text{m}$, the distance between the object and hologram planes $s = -1000 \text{ mm}$, the position of the reference source $s_r = -1600 \text{ mm}$ and $\alpha_r = 0.5^\circ$. The hologram width equal to 10 mm was assumed.

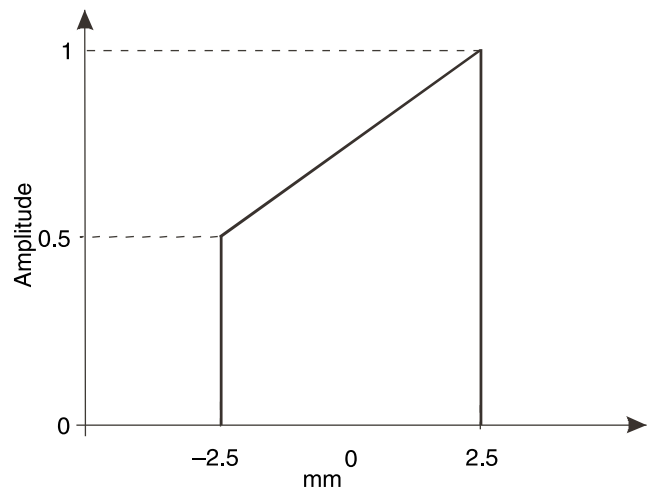


Fig. 4. Amplitude distribution of the registered object.

To receive more detailed field distribution at the hologram plane, the Fourier transformation was calculated for $N = 2^{16} = 65536$ samples. This means that outside of the object area the amplitude values were taken as equal to 0. Moreover, the ratio of the intensities of the reference and object beams was chosen to achieve the maximum modulation of the intensity distribution at the hologram plane.

Using the FFT procedure for N samples of a transformed function, its Fourier transform is received for the same number N of samples. According to the diffraction theory, if Δx_p is the distance between the adjacent pixels of the transformed function, then the distance Δx between the adjacent pixels of the Fourier transform can be found from the relation

$$\Delta x = \frac{|s|\lambda}{\Delta x_p N}, \quad (22)$$

where $|s|$ is the distance between the object and hologram spheres, see Fig. 3(a). The value Δx is indispensable to find the field distribution (number of the samples) registered on the hologram.

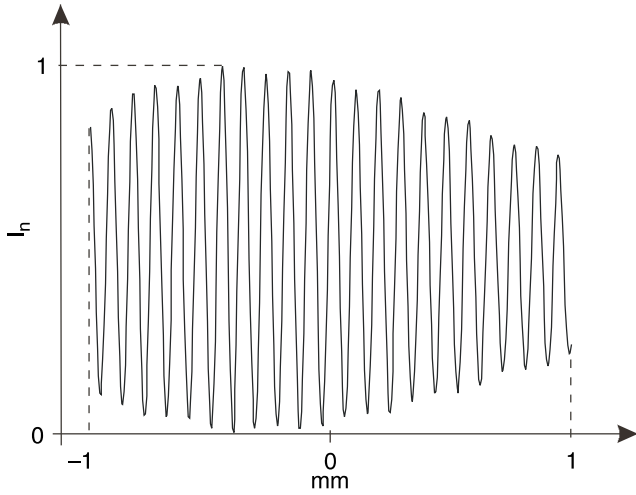


Fig. 5. Intensity distribution at central part of the hologram plane.

A general view of the central part of the intensity distribution at the hologram plane is shown in Fig. 5. The results were obtained with the aid of Eqs. (12)–(14). According to the Nyquist requirement every hologram fringe should be registered by at least two pixels. To verify the correctness of the registration process the diagram of the number of pixels for one fringe vs. the fringe number is shown in Fig. 6.

Using Eqs. (18), (19) and (20), the field distribution at an arbitrary plane located within the distance s' from the hologram plane can be obtained. The intensity distribution at the real image plane ($s' = s$), after removing the constant from the hologram field, is shown in Fig. 7. In this case the reconstruction source R' is coincident with the reference source R ($s'_r = s_r$, $\alpha'_r = \alpha_r$). Three typical components at the image plane are seen: real image, reconstruction source trace and defocused conjugate image. The transverse magnification of the real image is $\beta_r = s'/s = 1$ [7, Chapter 2] and from the theoretical point

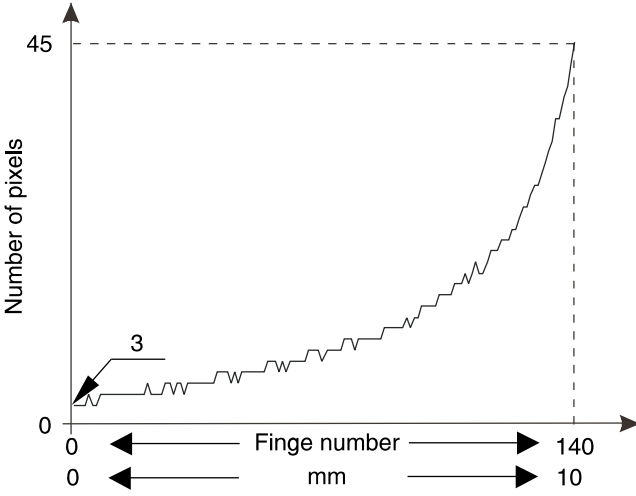


Fig. 6. Verification of Nyquist's condition. The diagram of number of pixels used for registration of individual fringes.

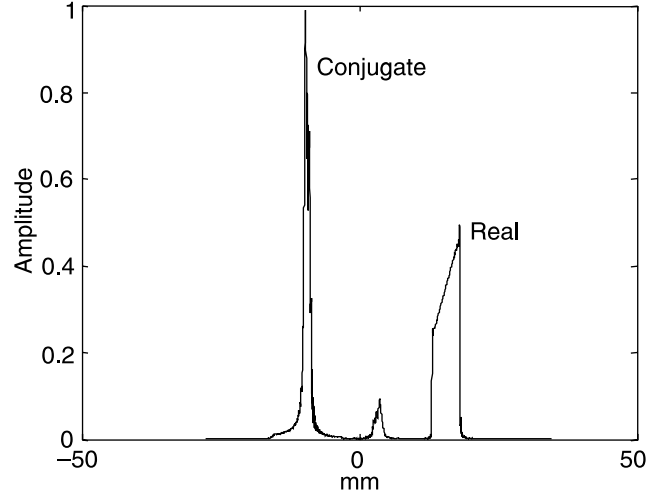


Fig. 7. Amplitude distribution at the real image plane of the Fresnel hologram.

of view the real image should be identical with the object. However, distinctly seen intensity oscillations and their sharp changes at the object edges (due to Gibbs' effect, [8]) are typical for the diffraction phenomenon related to limited hologram dimensions. When focusing on the conjugate image plane [$s' = ss_r/(2s-s_r) = -4000$] a sharp conjugate image and defocused real one are obtained [7]. Their forms are similar to real and conjugate images shown in Fig. 7, respectively. The word "similar" has been used to emphasise the change of the transverse magnification of the conjugate image equal to $\beta_c = -s'/s = -4^x$.

For the Fourier hologram, when the object and the reference sources are situated at the same plane ($s = s_r$) the real and conjugate images are situated at the plane coincident with the reconstruction source ($s' = s_r$). Such a situation is shown in Fig. 8. The transverse magnifications of the real and conjugate images are equal to $\beta = 1$ and $\beta_c = -1$, respectively.

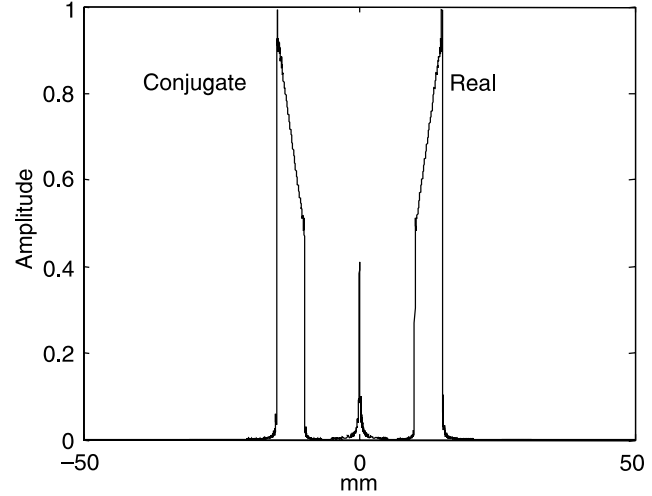


Fig. 8. Amplitude distribution at the real image plane of the Fourier hologram.

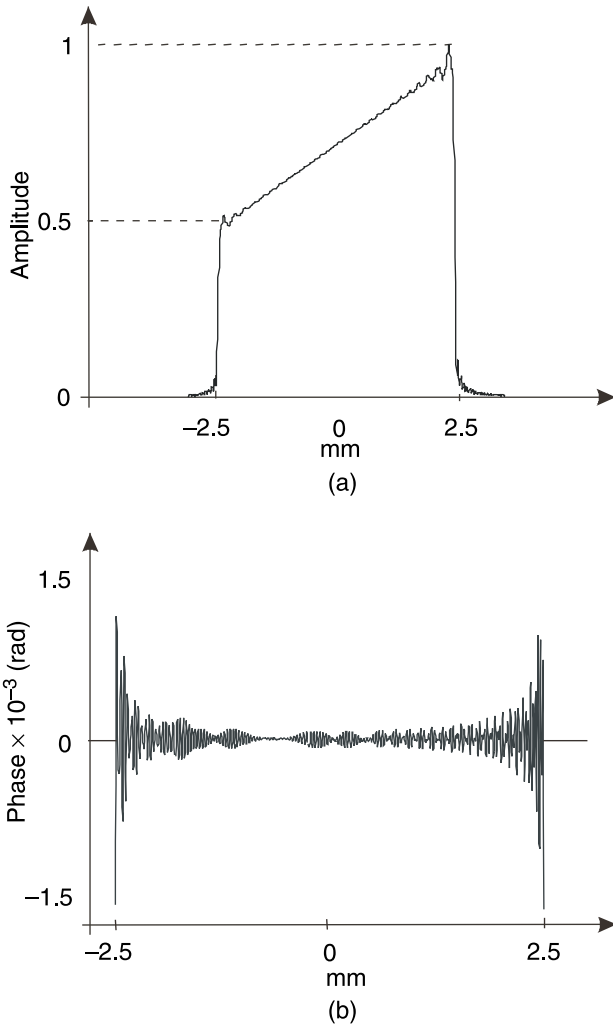


Fig. 9. Amplitude (a) and phase (b) distributions of separated real image area. The scale differences of image width are introduced for more clear presentation of the phase distribution oscillations.

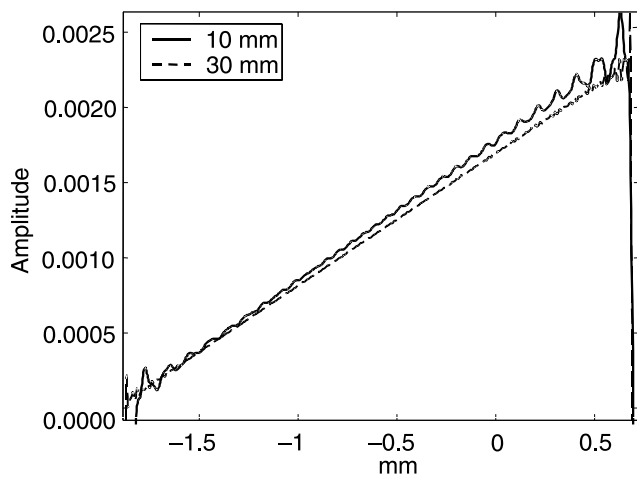


Fig. 10. Reconstruction amplitude for two different hologram sizes.

The amplitude and phase distributions for the separated real image in the case shown in Fig. 7 are shown in Fig. 9. The distributions for both the amplitude (a) and the phase (b) undergo distinct oscillations. As it was mentioned above such oscillations are encountered due to the limited hologram dimensions. They decrease with increasing the hologram dimensions. To demonstrate it, the holographic images for the hologram widths equal to 30 mm (dashed line) and 10 mm (solid line) are shown in Fig. 10. Intensity oscillations are observed outside the image of the object area as well. Additionally, at in many points the intensity value reaches zero, what leads to phase oscillation jumps between $-\pi$ and π . Therefore phase values in the object area are presented only [see Fig. 9(b)].

4. Image reconstruction from a laboratory hologram

The reconstruction procedures, Eqs. (17)–(21), were applied to hologram reconstruction of the object registered by the CCD camera. The experiment was done using holographic configuration shown in Fig. 11. The bolt shown in

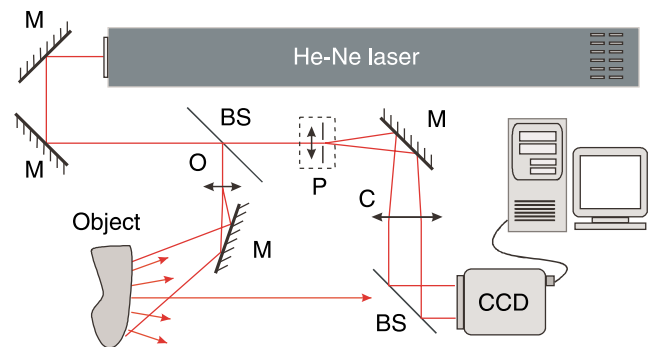


Fig. 11. Scheme of experimental arrangement used for digital hologram registration; M – mirror, BS – beam splitter, P – pinhole with focusing objective, O – imaging objective, C – collimator.

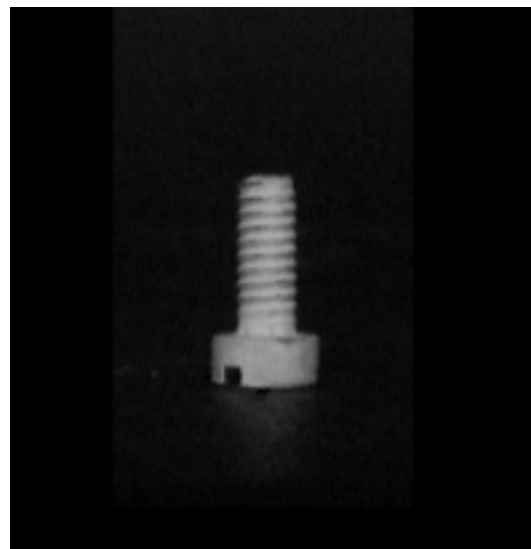
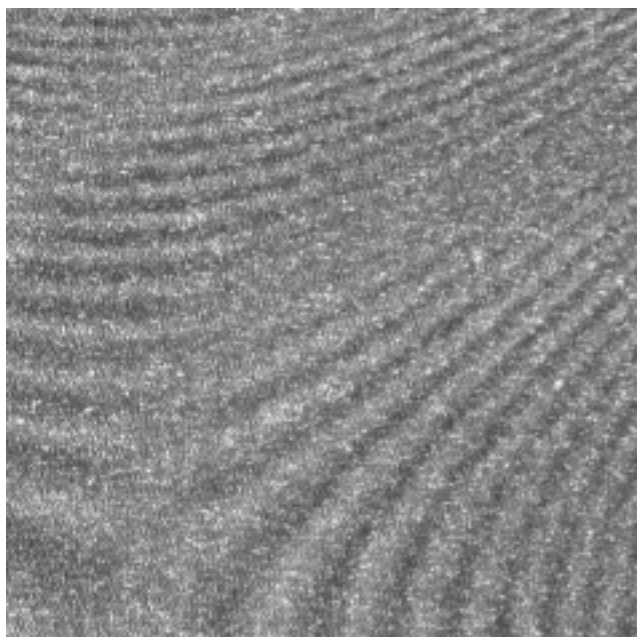


Fig. 12. Holographically registered object.



1024 × 1024 pixels

Fig. 13. Intensity distribution at the hologram plane.

Fig. 12 was located at the distance 600 mm from the surface of the CCD matrix. The reference beam collimated by the collimator C and reflected by the beam splitter impinges on the CCD matrix to interfere with the object beam. The fringe distribution registered by the camera is presented in Fig. 13. The intensity distribution at the hologram plane was sampled by 1024×1024 pixels. An example of the reconstructed real image is shown in Fig. 14. It is easy to observe that the image is surrounded by noise, formed by residues of the part of the zero diffraction order. It is worth to add that limited number of pixels reduces the quality of the reconstructed image due to the diffraction phenomena.

5. Conclusions

The analyses numerical results obtained prove that the sphere transformation theory applied to one-dimensional holographic process simulation as well as to the reconstruction of two-dimensional holograms is quite useful. The approach enables analysing various holographic configurations, namely, with different positions of the object, the reference and reconstruction sources and arbitrarily chosen image planes. Estimation of the influence of parameter differences between the reference and reconstruction beams on the holographic image quality is especially easy. The problem of the influence of beam aberrations at the registration stage will be the subject of the forthcoming paper.

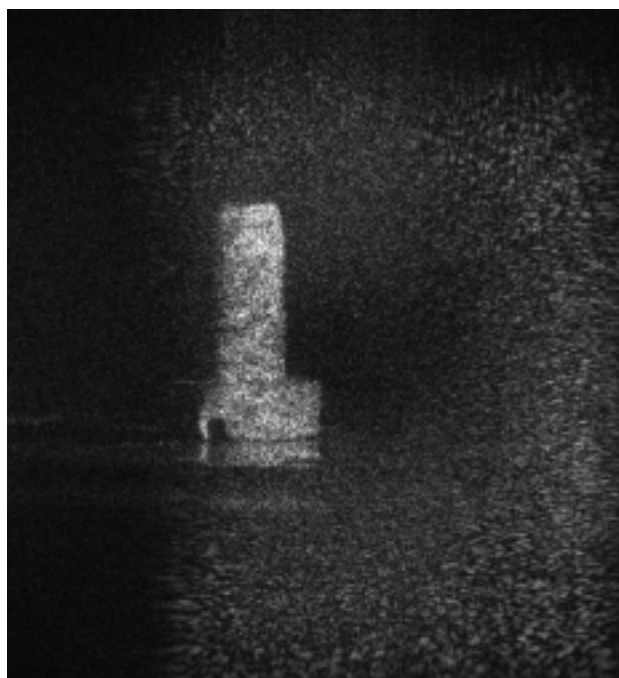


Fig. 14. Digitally reconstructed image.

References

1. M.A. Kronrod, N.S. Merzlyakov, and L.P. Yaroslavskii, "Reconstruction of a hologram with a computer," *Sov. Phys. Tech. Phys.* **17**, 333–334 (1972).
2. L.P. Yaroslavskii and N.S. Merzljakow, "Methods of digital holography," *Consultants Bureau*, New York, (1980).
3. T.M. Kreis and W.P.O. Jüptner, "Principles of digital holography," *Hybrid Measurement Technologies, Proc. 3rd Int. Workshop on Automatic Processing of Fringe Patterns (Fringe '97)*, Akademie Verlag, Berlin, 353–363 (1997).
4. T.M. Kreis, W.P.O. Jüptner, and J. Geldmacher, "Digital holography: methods and applications," *Proc. SPIE* **3407**, 169–177 (1998).
5. S. Paško and R. Jóźwicki, "Influence of Huygens-Kirchhoff formula approximations on image quality in digital holography," *Int. Conf. on Optical Holography and its Applications*, Kiev, 2000.
6. Jóźwicki, "Transformation of references spheres by an aberration free and infinitely large optical system in the Fresnel approximation," *Optica Acta* **29**, 1383–1393 (1982); "Distorter approach to wave optical imaging," *Research and Development Treatises*, Polish Chapter SPIE, Warsaw (1995).
7. J.Ch. Vienot, P. Smigielski, and H. Royer, *Holographie Optique. Developments-Applications*, Dunod, Paris, 1971, Ch. 2.
8. D.C. Champeney, *Fourier Transforms and their Physical Applications*, Academic Press, London, 1973, Ch. 1.

Forthcoming conferences

Readers are invited to send the Executive Editor details of conference to be announced

3–7 June

IEEE MTT-S International Microwave Symposium
Seattle, WA, USA
Web: www.ims2002.org

3–7 June

International Conference on MOVPE
Berlin, Germany
Web: icmovpe.physik.tu-berlin.de

17–21 June

European MRS Meeting
Strasbourg, France
Abstract deadline: 14 January
Web: www-emrs.c-strasbourg.fr

24–26 June

Device Research Conference (DRC)
Santa Barbara, CA, USA
Web: www.tms.org/Meetings/Specialty/DRC/2002/DRC-2002-Home.html

26–28 June

Electronic Materials Conference (EMC)
Santa Barbara, CA, USA
Web: www.tms.org/Meetings/Specialty/EMC02/EMC02.html

22–25 July

International Workshop on Nitride Semiconductors (IWNS)
Aachen, Germany
Abstract deadline: 10 March
Web: www.fz-juelich.de/iwn2002

4–8 August

14th American Conference on Crystal Growth and Epitaxy (ACCGE)
Seattle, WA, USA
Abstract deadline: 3 May
Web: www.crystalgrowth.org/conferences/accge14

6–8 August

IEEE Lester Eastman Conference on High Performance Devices
Newark, DE, USA
Abstract deadline: 14 April
Web: nina.ecse.rpi.edu/shur/EastmanConference

1–5 September

European Conf on Silicon Carbide and Related Materials (ECSCRM–2002)
Linköping, Sweden
Abstract deadline: 15 May
Web: www.ifin.liu.se/ecscrm2002

8–12 September

European Conference on Optical Communications (ECOC)
Copenhagen, Denmark
Abstract deadline: 15 April
Web: www.ecoc.dk

15–19 September

National Fiber-Optic Engineers Conference (NFOEC)
Dallas, TX, USA
Abstract deadline: 18 January
Web: www.nfoec.com

15–20 September

International MBE Conference
San Francisco, CA, USA
E-mail: harris@snowmass.stanford.edu

23–27 September

GAAS/European Microwave Week
Milan, Italy
Abstract deadline: 8 March
Web: www.eumw.com

29 September–1 October

Semiconductor Laser Conference
Garmisch, Germany
Abstract deadline: 1 May
Web: www.ileos.org/info/calendar2002.html

7–10 October

29th International Symposium on Compound Semiconductors (ISCS)
Lausanne, Switzerland
Abstract deadline: 15 May
Web: www.iscs2002.epfl.ch

21–23 October

GaAs 1C Symposium
Monterey, CA, USA
Web: www.gaasic.org

11–13 November

Compound Semiconductor Manufacturing Expo (CS-MAX)
San Jose, CA, USA
Web: www.cs-max.com

2–6 December

MRS Fall Meeting
Boston, MA, USA
Abstract deadline: 15 June
Web: www.mrs.org/meetings

2–6 December

International Electron Devices Meeting
Web: www.his.com/~iedm